

Supporting Information

A Long-Lived Azafullerenyl Radical Stabilized by Supramolecular Shielding with a [10]Cycloparaphenylene

Anastasios Stergiou, Jérémy Rio, Jan H. Griwatz, Denis Arčon, Hermann A. Wegner,*
Christopher P. Ewels,* and Nikos Tagmatarchis**

anie_201909126_sm_miscellaneous_information.pdf

Table of Contents

1. Materials	2
2. Methods	2
2.1. EPR measurements.....	2
2.2. DFT Calculations.	2-3
2.3. NMR measurements.....	3
3. EPR spectra (Figures S1-4).....	4-7
4. ¹ H NMR spectrum (Figure S5)	8
5. DFT structures (Figure S6)	9
6. DFT calculations (Tables S1-2)	10-11
References.....	11
Author Contributions	11

1. Materials

Aza[60]fullerene dimer, (C₅₉N)₂, was synthesized according to literature.^[7] C₆₀ was purchased from Bucky, USA. 1-Chloronaphthalene and other solvents and chemicals were purchased from Sigma-Aldrich and used as received. [10]CPP was purchased from TCI Europe and used as received.

Preparation of [10]CPP/(C₅₉N)₂ (2:1) in 1-chloronaphthalene for EPR spectroscopy. Briefly, (C₅₉N)₂ (3 mg, 2 μmol) was dissolved in 1-chloronaphthalene (0.3 mL) forming a transparent olive-green solution. [10]CPP (3 mg, 4 μmol) was dissolved in 1-chloronaphthalene (0.6 mL) forming a transparent bright yellow-greenish solution. The two solutions were mixed at rt under ambient conditions and were stirred for 8 h to allow efficient complexation (final concentration 2.3 mM).

2. Methods

2.1. EPR measurements

For the X-band (9.6 GHz) cw-EPR experiments, the solution was degassed by several freeze-pump-thaw cycles and then sealed under vacuum in a 4 mm diameter silica tube (Wilma Lab Glass). The Bruker E580 spectrometer was used together with a cylindrical TM₁₁₀ mode resonator ER 4103TM with a high-Q factor. In the experiments we used the modulation field of 0.01 mT. Sample was irradiated with a 532 nm light from the Brimrose laser (Model BRH-100-E) guided to the 50% transmission grid in the cavity with an optical fiber.

2.2. DFT Calculations

Calculations were performed using the density functional code AIMPRO^[2-4] by fitting the charge density plane waves with an energy cutoff of 300 Ha. Relativistic pseudopotentials generated by Hartwigsen, Goedecker and Hutter were used. 38 independent Gaussian-based functions were used as a basis set for carbon, 12 for hydrogen, and 40 for nitrogen. Periodic boundary conditions were used, the sizes chosen and checked to be sufficiently large to avoid interactions between molecules. Absolute energies were converged in the self-consistency cycle to better than 10⁻⁹ Ha. Atomic positions were geometrically optimized until the maximum atomic position change in a given iteration dropped below 10⁻⁹ a₀ (a₀: Bohr radius). Calculations were fully spin polarised with spin relaxation. Spin states of individual atoms were obtained using Mulliken population analysis. Diffusion barrier calculations were

obtained via climbing nudged elastic band between fully optimised end points. Hyperfine coupling parameters were calculated using core reconstruction with core corrections incorporated using perturbation theory.

2.3. NMR measurements

In a nitrogen-filled glove box the EPR glass-tube was opened and the solution was filtered. The precipitate was dissolved in dichloromethane. The solvent was evaporated under reduced pressure ($p = 10^{-2}$ mbar) to remove all remaining 1-chloronaphthalene for three days. The remaining solid was dissolved in CD_2Cl_2 .

The filtrate was also dried under reduced pressure ($p = 10^{-2}$ mbar) to remove all remaining 1-chloronaphthalene for seven days. The remaining solid was dissolved in CD_2Cl_2 .

^1H -NMR measurements of the samples were performed at 253 K with a Bruker Avance III HD 600 MHz NMR-spectrometer. ^1H -NMR measurement of 1-chloronaphthalene as reference was performed at 298 K with a Bruker Avance III HD 400 MHz NMR-spectrometer (see Fig S5).

3. EPR spectra (Figures S1-4)

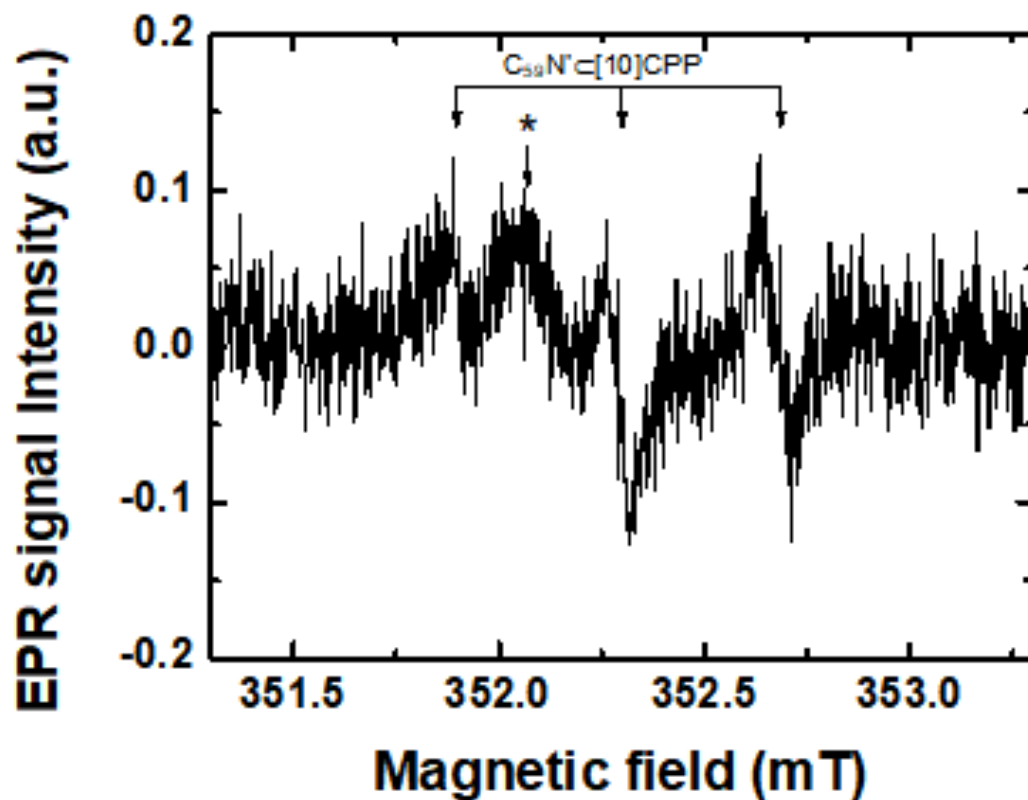


Figure S1. The X-band EPR spectrum of $C_{59}N[C10]CPP$ in 1-chloronaphthalene 300 min after switching-off the light illumination. The three peaks of residual $C_{59}N[C10]CPP$ are indicated with arrows and a trace signal at $g = 2.0025$ similar to that from $(C_{59}N)_2$ prior to illumination is marked with *.

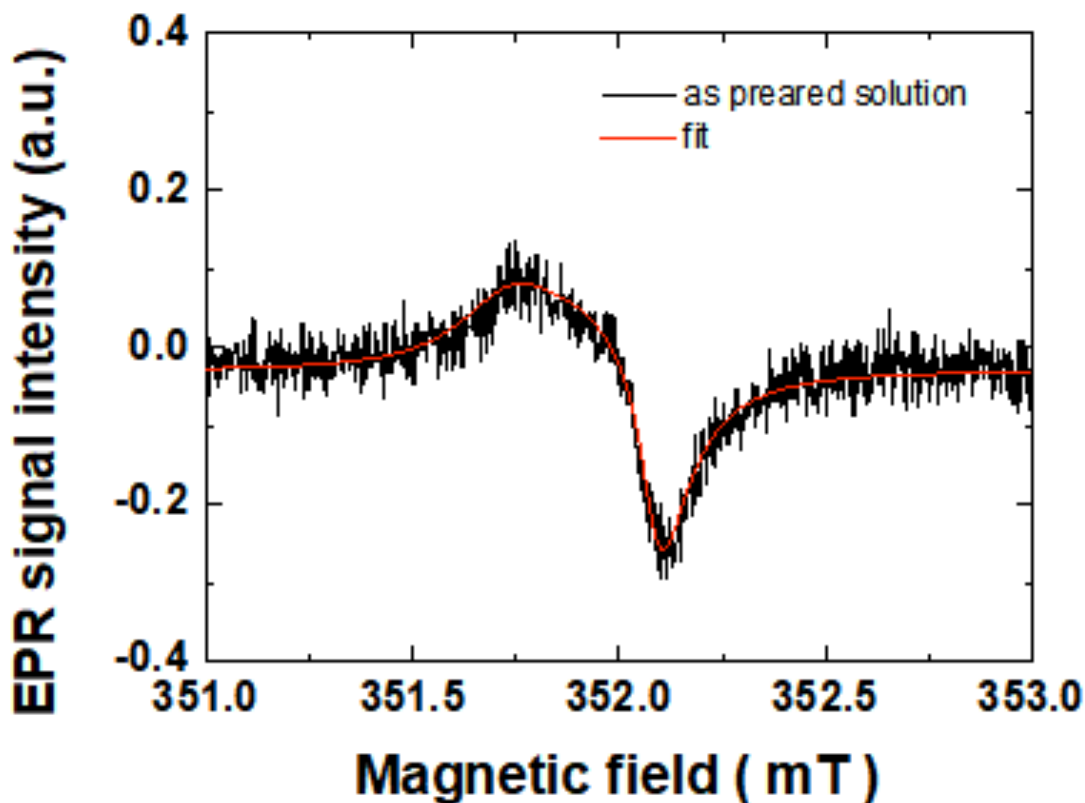


Figure S2. Room temperature X-band EPR spectrum of the as-prepared 1-chloronaphthalene solution containing [10]CPP and $(C_{59}N)_2$ in a 2:1 ratio (black). The line-shape fitting (red) yields the three eigenvalues $g_x = 2.0033$, $g_y = 2.0018$, $g_z = 2.0013$ and the average $g = 2.0021$.

The $[10]CPP \supset (C_{59}N)_2 \subset [10]CPP$ in 1-chloronaphthalene shows a weak X-band EPR signal (Fig. S2) with an average $g_{S1} = 2.0021$. Analogous trace signals are present in the studies of Dinse *et al.*^[5] prior photolysis, and can also be tracked in the studies by Wudl *et al.*^[6] during photolysis. The signal is possibly related to the distorted crystallinity of the sample as described by Kordatos *et al.*^[7] This signal cannot be due to unfunctionalized fulleride anions, C_{60}^{n-} ^[8-10] or due to other C_{60} -based impurities ($C_{60}O$ or $C_{120}O$) as they typically possess lower g -factors (i.e., less than 2).^[11] Since the g -factor of C_{60}^{*+} is just slightly larger than the free electron value of $g_e = 2.0023$,^[11,12] this possibility cannot be *a priori* excluded. However, the sample prior to the EPR experiment was first handled in air and as a result most C_{60}^{*+} centres should have already been eliminated and, therefore, this possibility is considered also unlikely. The measured g_{S1} implies a significant charge delocalisation. In fact, EPR signals at very similar g -factor values were previously reported for $C_{59}N^+ - C_{60}$ heterodimers^[13] and $C_{59}N^+ - C_{59}HN$ homodimers^[14] in solid state. Therefore, we suggest that the featureless trace signals prior and after illumination are not related to charge exchange between the $C_{59}N^+$ and the [10]CPP species but are rather originating from the fullerene species alone.

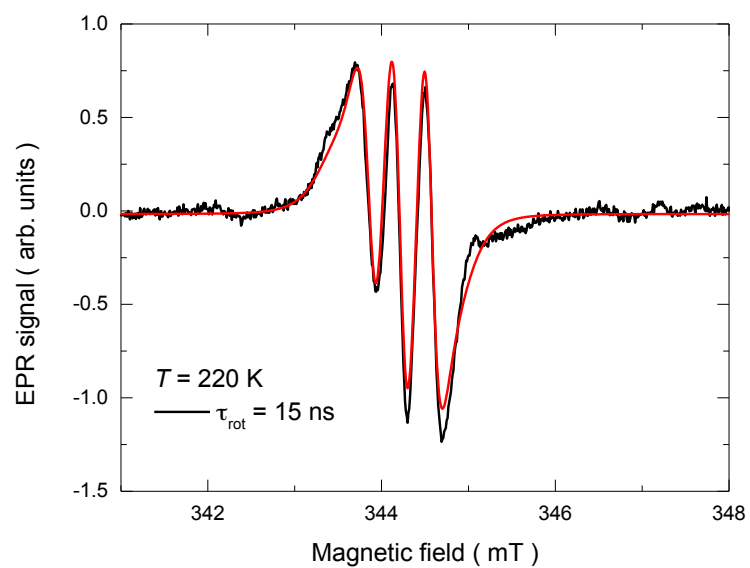


Figure S3. X-band cw EPR spectrum measured at 220 K (black line) together with the line-shape simulation (thick red line) in a limit of slow isotropic rotations.

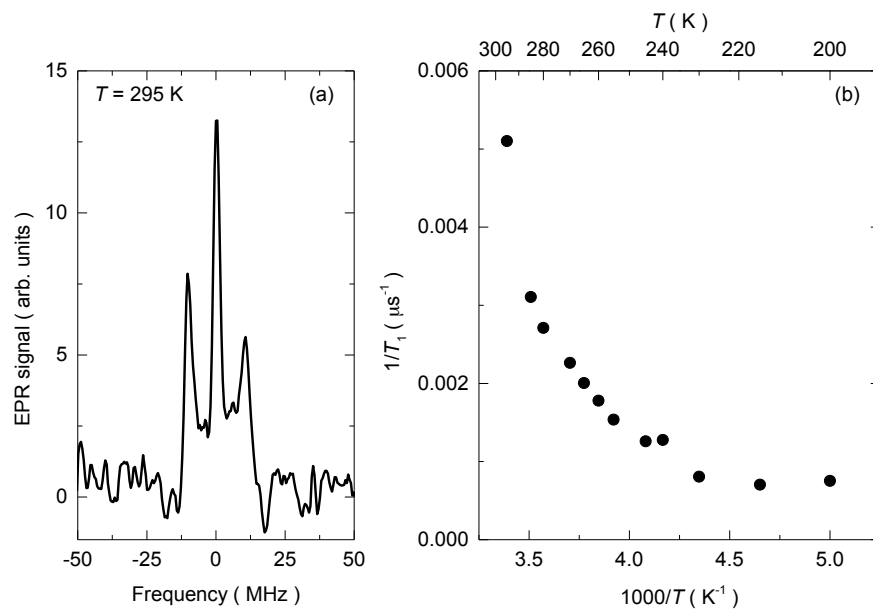


Figure S4. X-band cw EPR spectrum measured at 220 K (black line) together with the line-shape simulation (thick red line) in a limit of slow isotropic rotations.

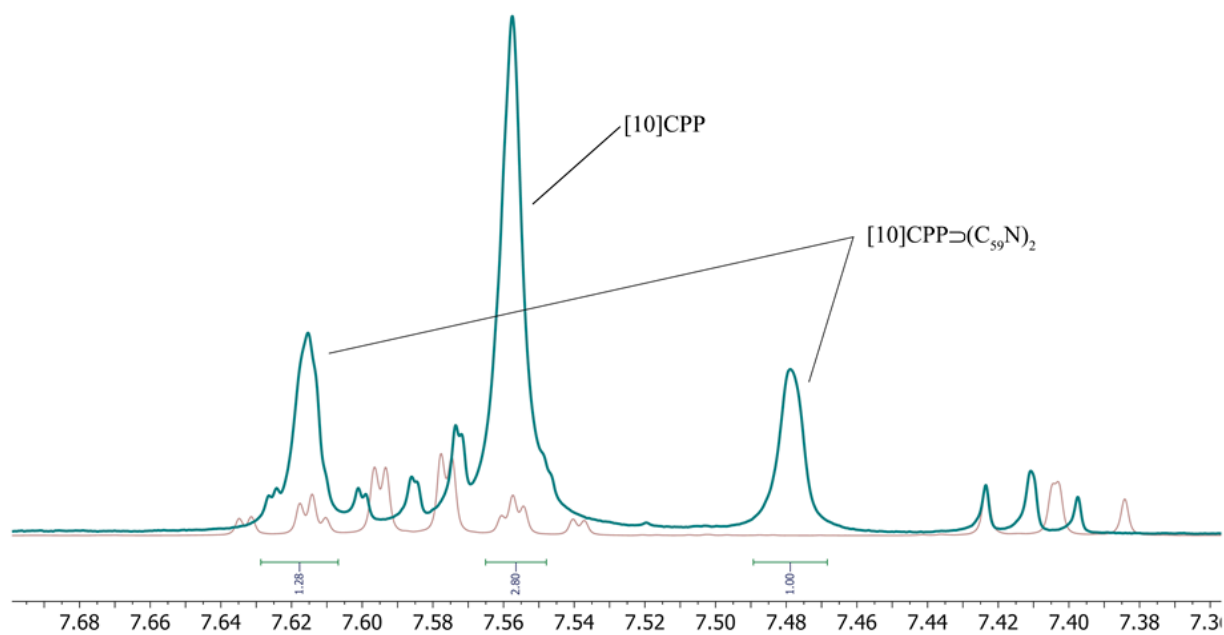
4. ^1H NMR spectrum (Figure S3)

Figure S5. ^1H -NMR spectrum obtained in CD_2Cl_2 for the precipitated $[10]\text{CPP}\supset(\text{C}_{59}\text{N})_2$ complex isolated after irradiation of the 2:1 molar ratio of $[10]\text{CPP}$ and $(\text{C}_{59}\text{N})_2$ in 1-chloronaphthalene (green). ^1H -NMR spectrum of 1-chloronaphthalene in CD_2Cl_2 as reference (brown).

5. DFT structures (Figure S6)

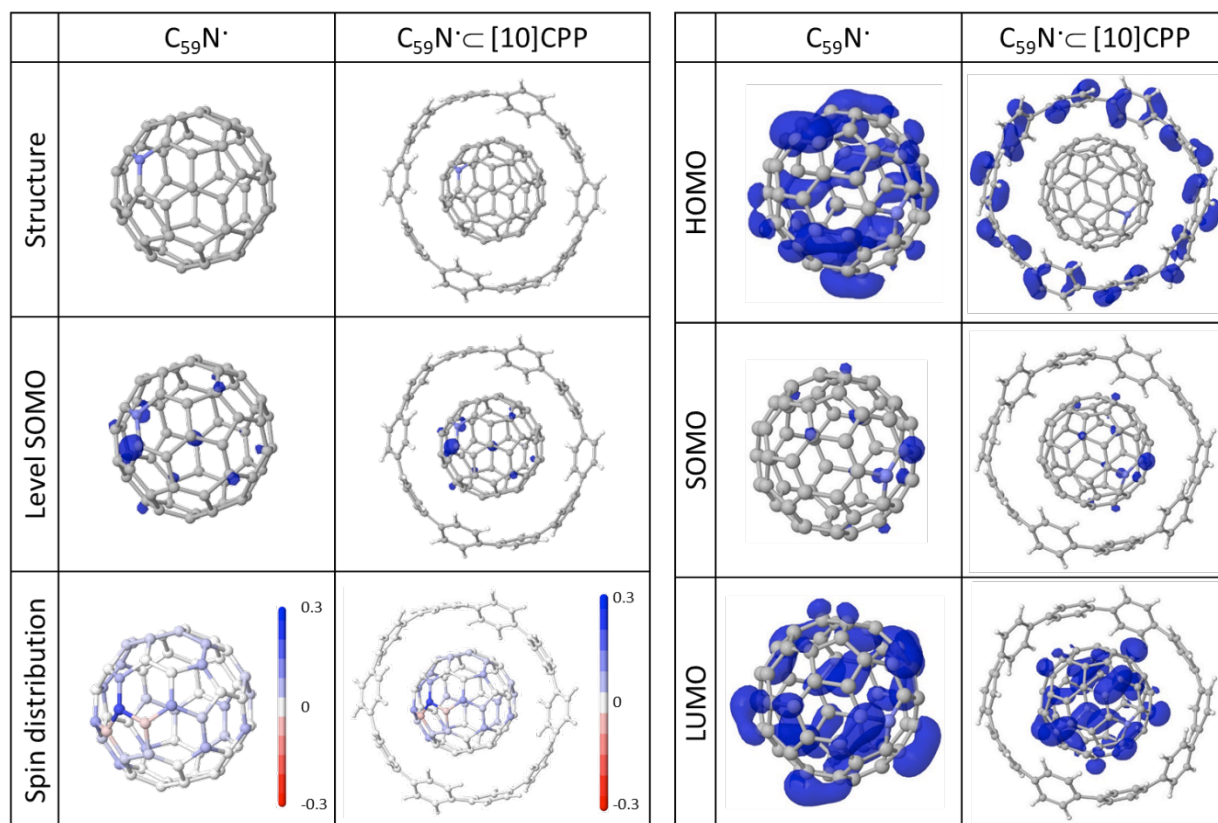


Figure S6. Left panel: DFT calculated stable structure for $C_{59}N^{\cdot}$ and $C_{59}N^{\cdot} \subset [10]CPP$ showing distribution of the unpaired singly occupied molecular orbital (SOMO) level, as well as total system spin (difference between spin-up and spin-down charge density). Both show that spin is almost exclusively localized on the carbon radical neighbouring the substitutional nitrogen, and is essentially unperturbed by the presence of the [10]CPP. Right panel: Wavefunction distribution squared for the highest occupied molecular orbital (HOMO), SOMO and lowest unoccupied molecular orbital (LUMO) for $C_{59}N^{\cdot}$ and $C_{59}N^{\cdot} \subset [10]CPP$, showing the [10]CPP HOMO lies above that of $C_{59}N^{\cdot}$.

6. DFT calculations (Tables S1-2)

Table S1. DFT calculated hyperfine splitting parameters for $C_{59}N'$ and $C_{59}N' \square [10]CPP$ showing the principle values (MHz) and directions, followed by the conventional isotropic hyperfine parameter (MHz). Calculations are performed for the substitutional nitrogen (^{14}N) and for ^{13}C on its three neighbour sites, including the neighbouring radical carbon.

	<i>Isolated $C_{59}N'$</i>	<i>$C_{59}N' \square [10]CPP$</i>
^{14}N	Principal values and direction 6.74 (0.379, 0.338, 0.861) 6.76 (0.742, -0.667, -0.064) 19.28 (-0.553, -0.664, 0.504) Conventional Isotropic: 10.92	Principal values and direction 6.01 (0.525, 0.200, 0.827) 6.04 (0.647, -0.725, -0.236) 17.88 (-0.552, -0.659, 0.510) Conventional Isotropic: 9.97
Radical ^{13}C	Principal values and direction 32.02 (0.634, -0.0773, 0.036) 32.38 (0.372, 0.344, 0.862) 82.17 (-0.679, -0.533, 0.505) Conventional Isotropic: 48.74	Principal values and direction 31.02 (0.652, -0.754, 0.081) 31.38 (0.335, 0.383, 0.861) 79.49 (-0.680, -0.534, 0.502) Conventional Isotropic: 47.18
Two back-bonded ^{13}C neighbours	Principal values and direction -4.70 (-0.504, -0.827, 0.249) -3.53 (-0.798, 0.335, -0.501) -1.83 (-0.331, 0.451, 0.829) Conventional Isotropic: -3.45, -3.47	Principal values and direction -4.07 (0.283, 0.654, -0.702) -3.16 (0.332, -0.753, -0.568) -1.49 (-0.900, -0.073, -0.430) Conventional Isotropic: -3.21, -3.75

Table S2. DFT calculated relative enthalpies (eV) of different stages in [10]CPP catalyzed separation and stabilization of radicals from $(C_{59}N)_2$. The process is shown in detail in Figure 3 of the main paper. When ranges are given, this corresponds to the orientational freedom of $C_{59}N^{\cdot}$ within the [10]CPP.

Species	Relative Enthalpy (eV)
$(C_{59}N)_2 \subset [10]CPP + [10]CPP$ (ground state)	0.000
$(C_{59}N)_2 \subset [10]CPP + [10]CPP$ (triplet state)	+0.870
$C_{59}N^{\cdot} \subset [10]CPP + C_{59}N^{\cdot} + [10]CPP$	+1.974 to +1.652
$2 C_{59}N^{\cdot} \subset [10]CPP$	+0.830 to +0.185
$[10]CPP \supset (C_{59}N)_2 \subset [10]CPP$	-3.042

References

- [1] J. C. Hummelen, B. Knight, J. Pavlovich, R. González, F. Wudl, *Science* **1995**, 269, 1554.
- [2] P. R. Briddon, R. Jones, *Phys. Status Solidi (b)* **2000**, 217, 131-171.
- [3] M. J. Rayson, P. R. Briddon, *Phys. Rev. B* **2009**, 80, 205104.
- [4] P. R. Briddon, M. J. Rayson, *Phys. Status Solidi (b)* **2011**, 248, 1309-1318.
- [5] A. Gruss, K.-P. Dinse, A. Hirsch, B. Nuber, U. Reuther, *J. Am. Chem. Soc.* **1997**, 119, 8728-8729.
- [6] K. Hasharoni, C. Bellavia-Lund, M. Keshavarz-K, G. Srdanov, F. Wudl, *J. Am. Chem. Soc.* **1997**, 119, 11128-11129.
- [7] H. Kuzmany, J. Fink, M. Mehring, S. Roth, in *Molecular Nanostructures 1-570* (WORLD SCIENTIFIC, 1998).
- [8] M. R. Wasielewski, M. P. O'Neil, K. R. Lykke, M. J. Pellin, D. M. Gruen, *J. Am. Chem. Soc.* **1991**, 113, 2774-2776.
- [9] M. M. Khaled, R. T. Carlin, P. C. Trulove, G. R. Eaton, S. S. Eaton, *J. Am. Chem. Soc.* **1994**, 116, 3465-3474.
- [10] A. J. Schell-Sorokin, F. Mehran, G. R. Eaton, S. S. Eaton, A. Viehbeck, T. R. O'Toole, C. A. Brown, *Chem. Phys. Lett.* **1992**, 195, 225-232.
- [11] P. Paul, K.-C. Kim, D. Sun, P. D. W. Boyd, C. A. Reed, *J. Am. Chem. Soc.* **2002**, 124, 4394-4401.
- [12] S. G. Kukolich, D. R. Huffman, *Chem. Phys. Lett.* **1991**, 182, 263-265.
- [13] A. Rockenbauer, G. Csányi, F. Fülöp, S. Garaj, L. Korecz, R. Lukács, F. Simon, L. Forró, S. Pekker, A. Jánosy, *Phys. Rev. Lett.* **2005**, 94, 066603.
- [14] D. Arçon, M. Pregelj, P. Cevc, G. Rotas, G. Pagona, N. Tagmatarchis, C. Ewels, *Chem. Commun.* **2007**, 3386-3388.

Author Contributions

A.S. prepared the samples and carried out some EPR measurements under the guidance of D.A. D.A. conceived the EPR measurements and performed the analysis of the data. C.E. and J.R. conceived, performed and analysed the theoretical calculations. J.H.G. and H.A.W. designed the NMR measurements and performed the analysis of the data. N.T., C.E., H.A.W. and D.A. designed the project, supervised the work and discussed the data. All authors interpreted the data and contributed to the preparation of the manuscript.